

## Interplay of halogen and hydrogen bonding in a series of heteroleptic iron(III) complexes

**Authors:** Raúl Díaz-Torres,<sup>1</sup> Jorge Echeverría,<sup>2</sup> Oliver Loveday,<sup>2</sup>  
Phimphaka Harding\*<sup>1</sup> and David J. Harding\*<sup>1</sup>

<sup>1</sup> Functional Materials and Nanotechnology Centre of Excellence, Walailak University,  
Thasala, Nakhon Si Thammarat, 80160, Thailand.

<sup>2</sup> Departament de Química Inorgànica i Orgànica & IQTC-UB, Universitat de Barcelona,  
Martí i Franquès, 1-11, 08028 Barcelona, Spain.

E-mail: [hdavid@mail.wu.ac.th](mailto:h david@mail.wu.ac.th) or [kphimpha@mail.wu.ac.th](mailto:kphimpha@mail.wu.ac.th)

[www.funtechwu.com](http://www.funtechwu.com)

Twitter: @GroupHarding

## Table of Contents

	Page No.
<b>Figure S1</b> UV-Visible spectra of <b>4</b> in DCM and DMF at 0.001 M.	3
<b>Figure S2</b> ATR-IR spectra for <b>1-4</b> .	3
<b>Table S1</b> Crystallographic data and structure refinement of <b>1-4</b> .	6
<b>Table S2</b> Intermolecular interactions of <b>1-4</b> (Å).	7
<b>Figure S3</b> Experimental PXRD diffractograms and the corresponding simulated patterns for <b>1-4</b> at room temperature.	8
<b>Figure S4</b> Cross-section of the 1D chain for <b>1</b> (square) and <b>4</b> (rectangular).	10
<b>Figure S5</b> Structural representation of the supramolecular $\pi$ - $\pi$ and C-H $\cdots$ O contacts connecting the planes of Fe(III) centers in <b>1</b> .	10
<b>Figure S6</b> Structural representation of the supramolecular O $\cdots$ I interactions connecting the planes of Fe(III) centers in <b>4</b> .	11
<b>Figure S7</b> Hirshfeld surface 2D fingerprint plots: all contacts, H $\cdots$ X, O $\cdots$ X, H $\cdots$ H and O $\cdots$ H for <b>1-4</b> .	12
<b>Table S3</b> Intermolecular interactions contributions for <b>1-4</b> calculated by Hirshfeld surface.	12
<b>Table S4</b> QTAIM parameters at the bond critical points for the different dimers in the crystal structures <b>1-4</b> . All values are given in a.u.	13
<b>Figure S8</b> Cyclic voltammogram (Fe <sup>3+</sup> /Fe <sup>2+</sup> redox peak) of <b>1-4</b> at different scan rates and the representation of $i_p$ vs $v^{1/2}$ .	14
<b>Table S5</b> Electrochemical properties of <b>1-4</b> .	15
<b>Figure S9</b> Cyclic voltammogram of <b>4</b> in DCM containing 0.1 M of TBAPF <sub>6</sub> (scan rate 50 mV/s) vs Fc/Fc <sup>+</sup> .	16
<b>Figure S10</b> Cyclic voltammogram of Hqsal-I in DCM containing 0.1 M of TBAPF <sub>6</sub> (scan rate 50 mV/s) vs Fc/Fc <sup>+</sup> .	16
<b>Figure S11</b> Plot of $E'^{\circ}$ (V) vs $\sigma_p$ for <b>1-4</b> .	17

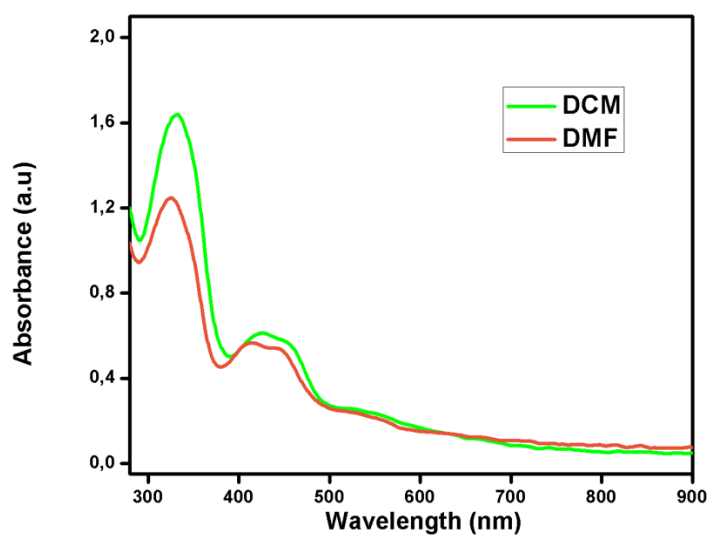
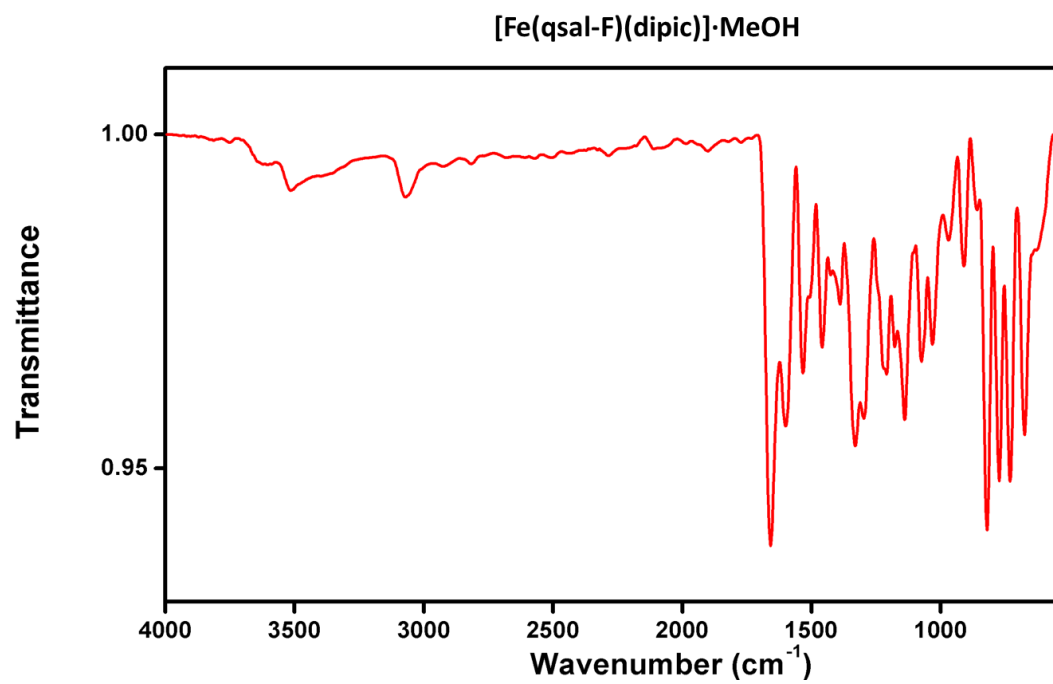
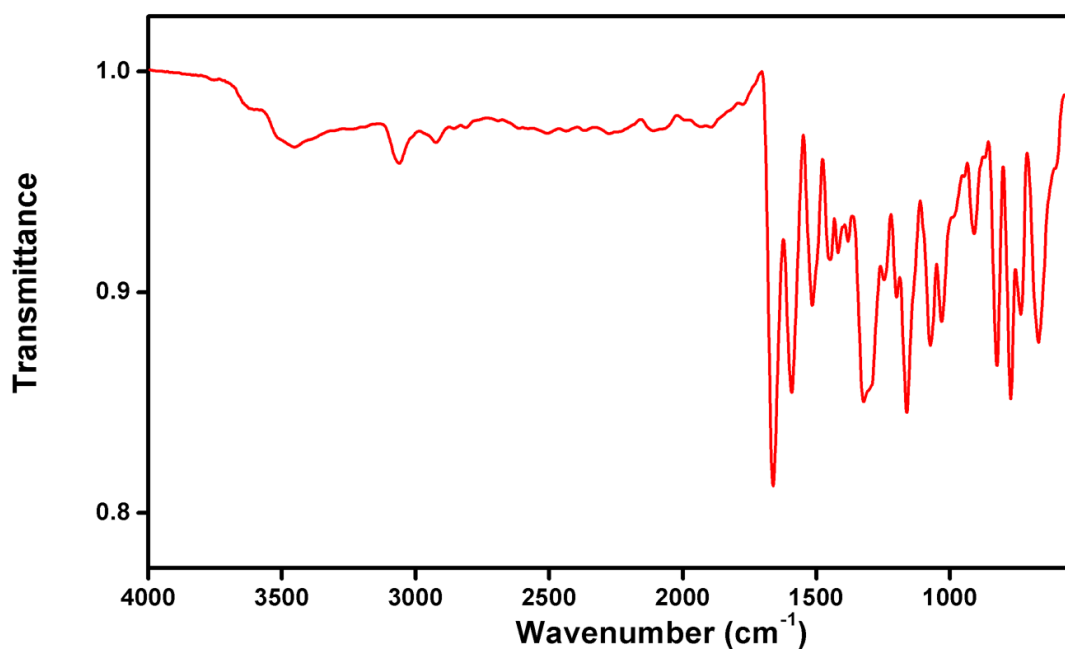


**Figure S1** UV-Visible spectra of **4** in DCM (green) and DMF (orange) at 0.001 M.

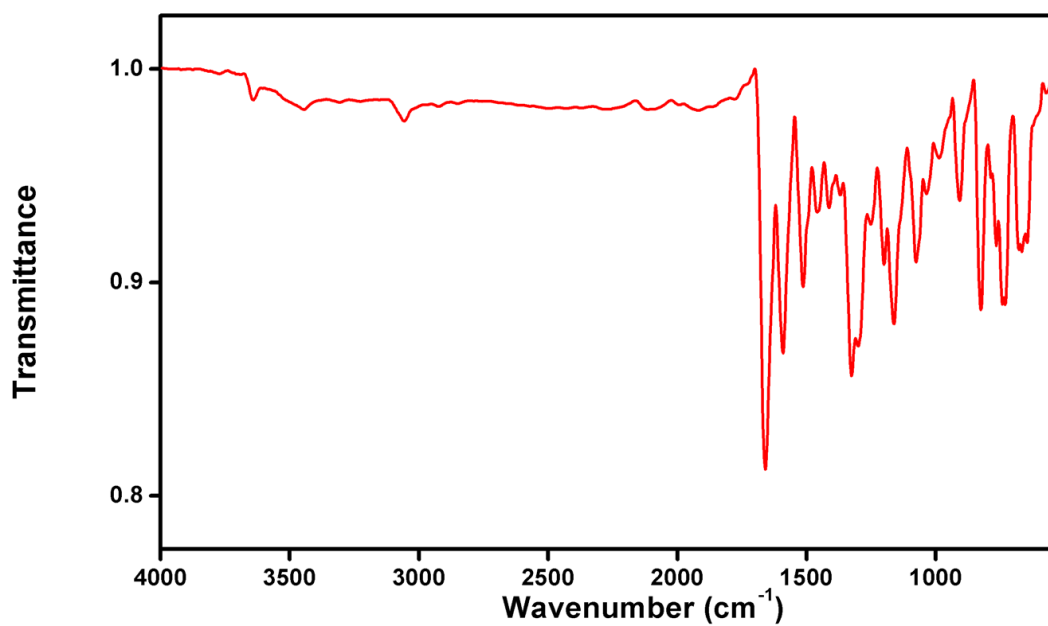
#### ATR-IR spectra



[Fe(qsal-Cl)(dipic)]·MeOH



[Fe(qsal-Br)(dipic)]·MeOH



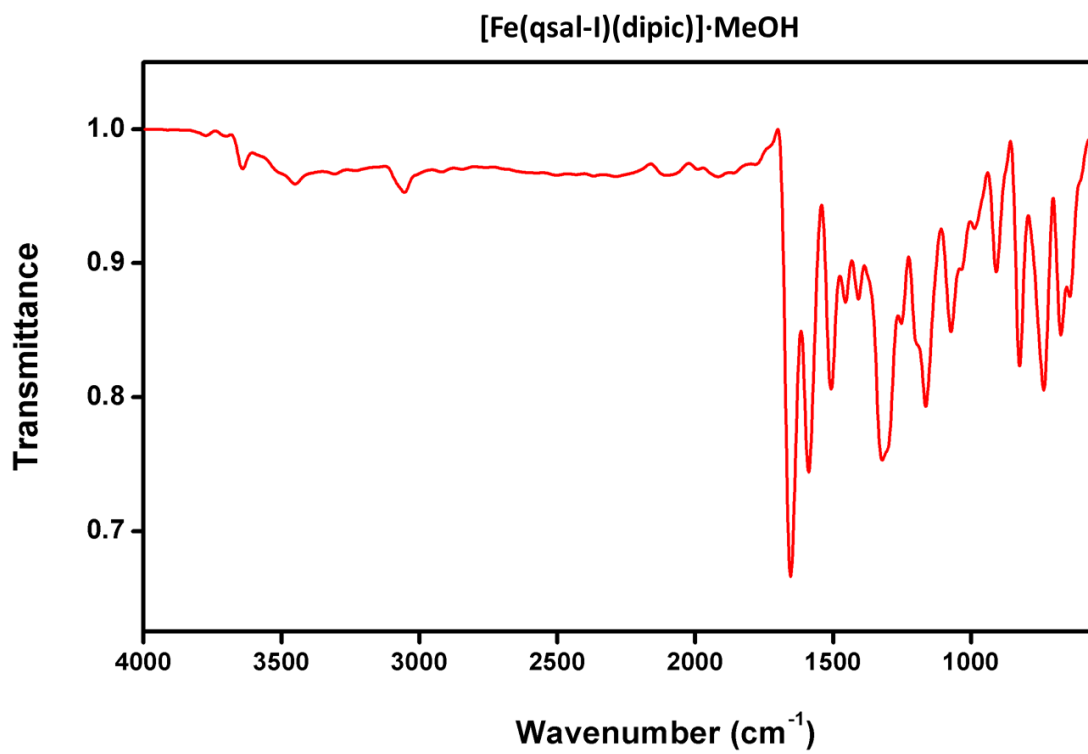


**Figure S2** ATR-IR spectra for **1-4**.

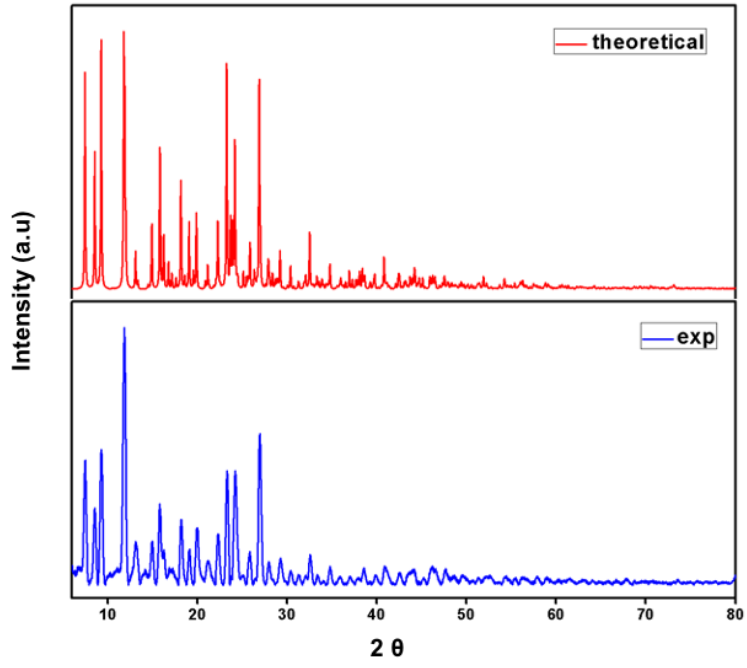
**Table S1** Crystallographic data and structure refinement of **1-4**.

<b>[Fe(qsal-X)(dipic)]·MeOH</b>				
	<b>F</b>	<b>Cl</b>	<b>Br</b>	<b>I</b>
Empirical formula	C <sub>24</sub> H <sub>17</sub> FFeN <sub>3</sub> O <sub>6</sub>	C <sub>24</sub> H <sub>17</sub> ClFeN <sub>3</sub> O <sub>6</sub>	C <sub>24</sub> H <sub>17</sub> BrFeN <sub>3</sub> O <sub>6</sub>	C <sub>24</sub> H <sub>17</sub> IFeN <sub>3</sub> O <sub>6</sub>
Formula weight/ gmol <sup>-1</sup>	518.26	534.70	579.16	626.15
Crystal system	triclinic	triclinic	monoclinic	monoclinic
Space group	<i>P</i> $\bar{1}$	<i>P</i> $\bar{1}$	<i>P</i> 2 <sub>1</sub> / <i>n</i>	<i>P</i> 2 <sub>1</sub> / <i>n</i>
a / Å	8.1982(3)	8.2215(2)	12.20560(10)	12.1991(2)
b / Å	11.5358(5)	11.9651(3)	9.30670(10)	9.3756(2)
c / Å	12.9597(6)	12.8982(3)	18.8067(2)	19.0747(4)
α / °	103.868(4)	105.940(2)	90	90
β / °	103.308(4)	105.557(2)	94.8010(10)	95.6028(19)
γ / °	107.779(4)	104.264(2)	90	90
Cell volume / Å <sup>3</sup>	1070.33(9)	1102.95(5)	2128.83(4)	2171.23(8)
Z	2	2	4	4
Absorption coefficient / mm <sup>-1</sup>	6.168	7.027	8.326	17.172
Reflections collected	15309	16928	17206	17238
Independent reflections, R <sub>int</sub>	3880, 0.0798	4030, 0.0546	3905, 0.0782	3969
Max. and min. transmission	0.736 / 0.202	0.743 / 0.397	1.000 / 0.734	0.526 / 0.232
Restraints/parameters	0/ 318	36/ 318	0/ 318	0/ 318
Final R indices [I>=2σ (I)]				
R <sub>1</sub> , wR <sub>2</sub>	0.0686, 0.1762	0.0813, 0.2119	0.0489, 0.1237	0.0675, 0.1704
CCDC No.	2075294	2075296	2075295	2075297

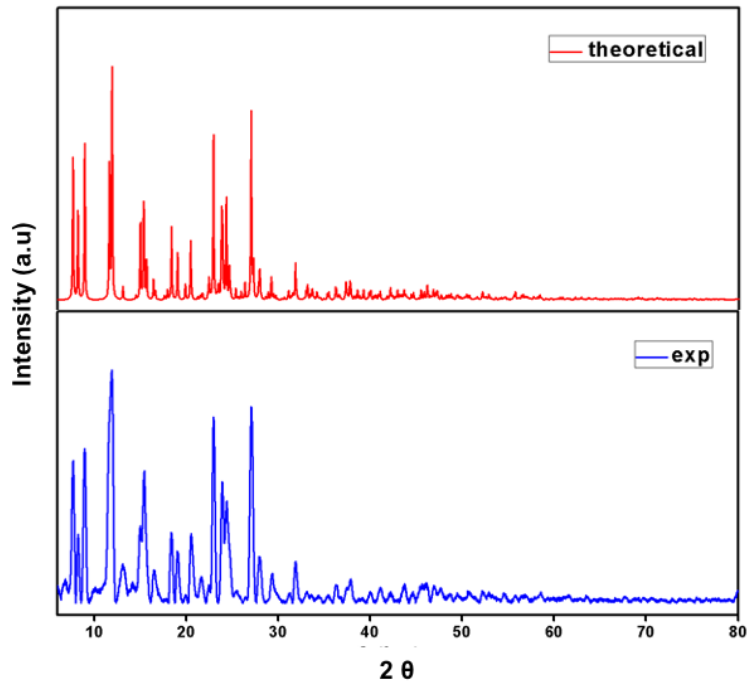
**Table S2** Intermolecular interactions of **1-4** (Å).

		<b>F</b>	<b>Cl</b>	<b>Br</b>	<b>I</b>
<b>1D chain</b>					
<b>C-H...O</b>					
	O1-H21	2.587	2.582	2.686	2.711
	O2-H10	2.472	2.541	2.643	2.497
<b><math>\pi</math>-<math>\pi</math></b>					
Quinoline	centroid-centroid	3.794	3.696	3.668	3.710
Dipic	centroid-centroid	-	-	3.553	3.567
<b>C=O...<math>\pi</math></b>					
dipic	atom-atom	3.322	3.350	-	-
<b>Fe-Fe</b>					
dipic		7.529	7.466	7.691	7.707
quinoline		6.756	6.769	7.061	7.087
<b>2D and 3D</b>					
<b><math>\pi</math>-<math>\pi</math></b>					
Quinoline	centroid-centroid	3.771	3.525	3.575	3.585
<b>C-H...O</b>					
dipic-quin	O5-H5	2.662	2.576	2.662	2.675
X...H	X1-H1	2.437	2.844	3.008	3.058
X... $\pi$	X1-C21	-	3.422	-	3.632
X...O	X1-O5	-	-	3.166	3.151
OH...CH	H6A-O5	1.930	1.831	2.236	2.261

1



2





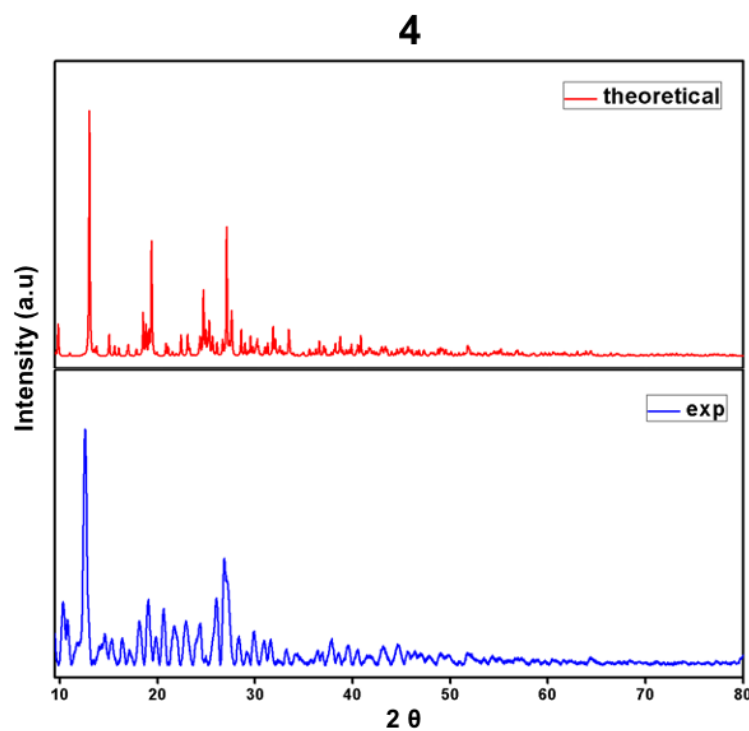
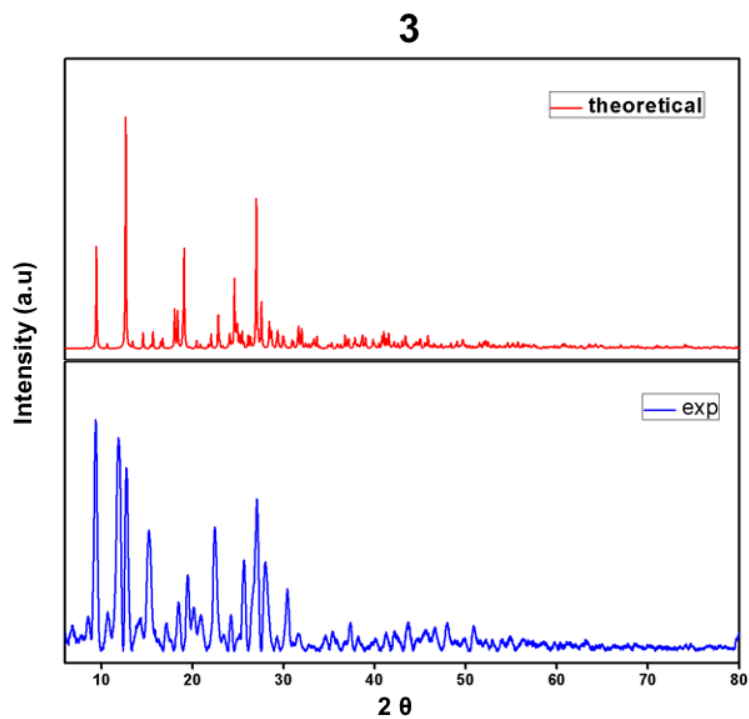


**Figure S3** Experimental PXRD diffractograms (blue) and the corresponding simulated patterns (red) for **1-4** at room temperature.

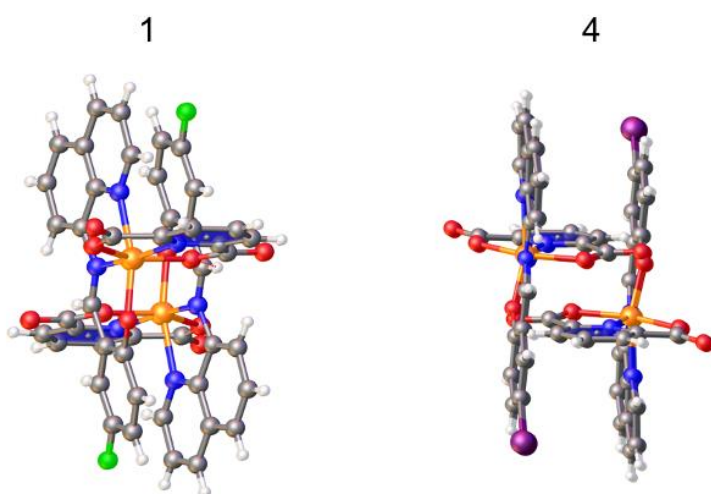


**Figure S4** Cross-section of the 1D chain for **1** (square) and **4** (rectangular).

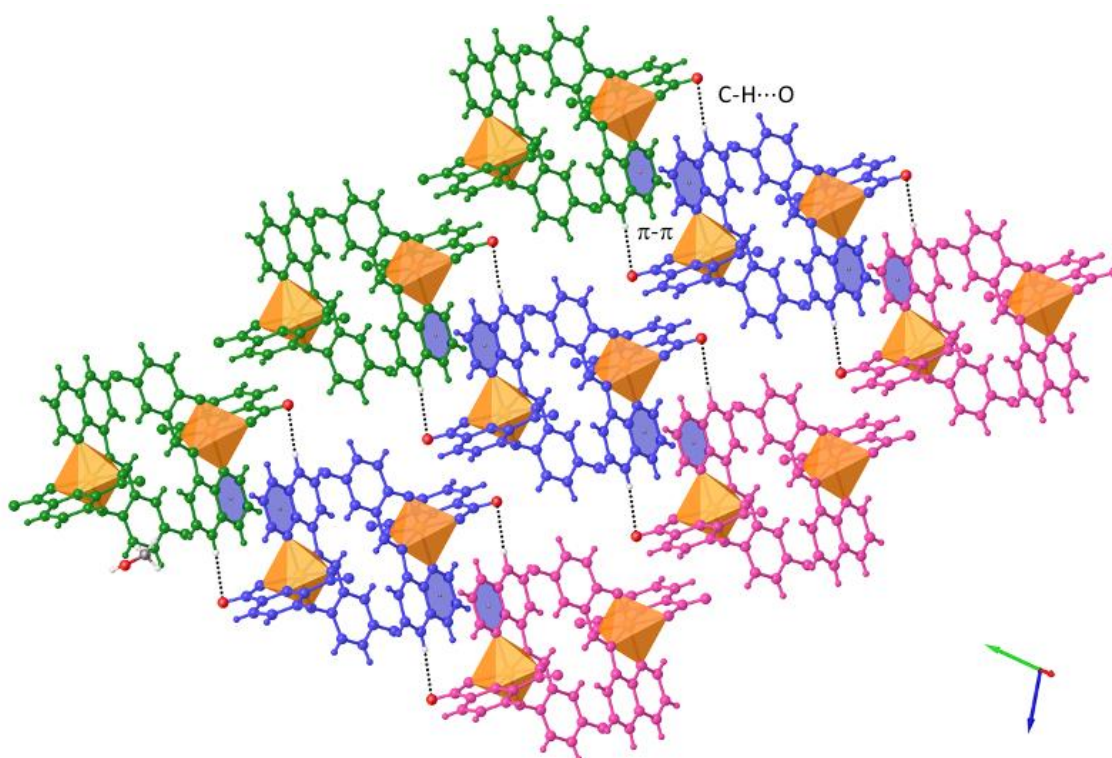


**Figure S5** Structural representation of the supramolecular  $\pi$ - $\pi$  and C-H...O contacts connecting the planes of Fe(III) centers in **1**.

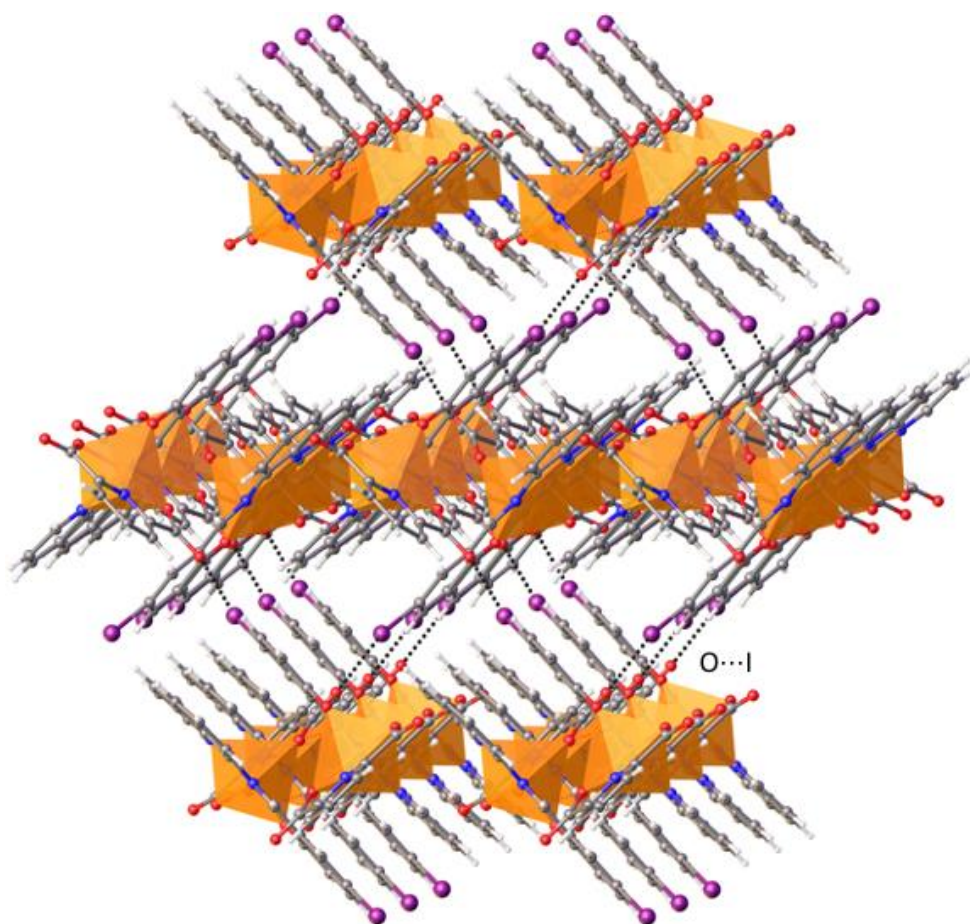


**Figure S6** Structural representation of the supramolecular O...I interactions connecting the planes of Fe(III) centers in **4**.

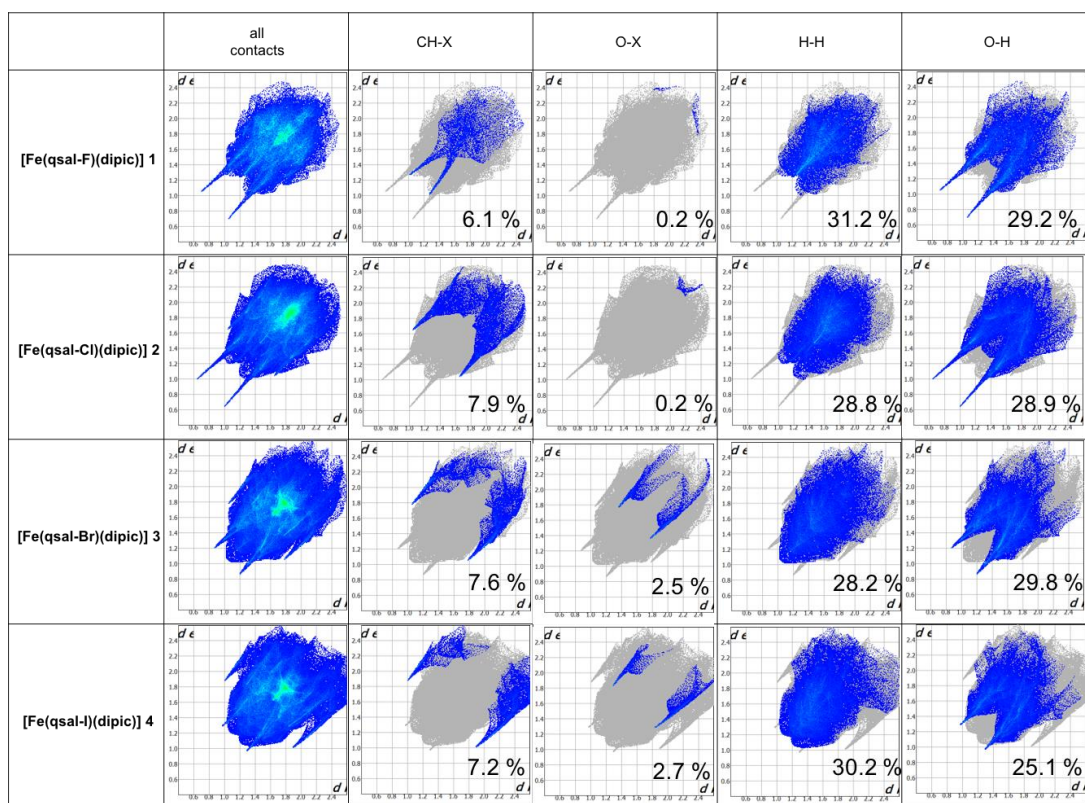


**Figure S7** Hirshfeld surface 2D fingerprint plots: all contacts, C-H...X, O...X, H...H and O...H for **1-4**.

**Table S3** Intermolecular interactions contributions for **1-4** calculated by Hirshfeld surface.

	H...H	CH...X	H...O	H...C	O...X	C...C	C...X	H...N	Other
<b>1</b>	31.2	6.1	29.2	14.7	0.2	9.0	3.2	1.6	4.8
<b>2</b>	28.8	7.9	28.9	15.2	0.2	8.2	4.1	1.7	5.0
<b>3</b>	28.2	7.6	29.8	12.0	2.5	9.0	3.2	1.9	5.6
<b>4</b>	30.2	7.2	25.1	16.0	2.7	8.3	3.0	1.9	5.8

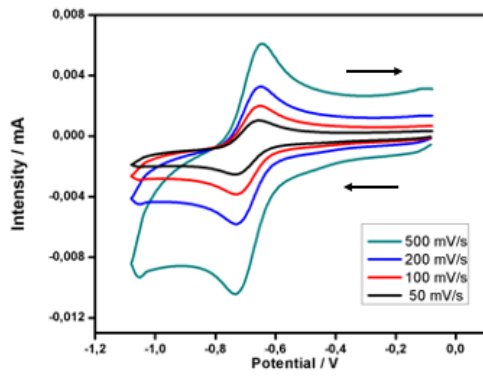
## Theoretical Results

**Table S4.** QTAIM parameters at the bond critical points for the different dimers in the crystal structures **1-4**. All values are given in a.u.

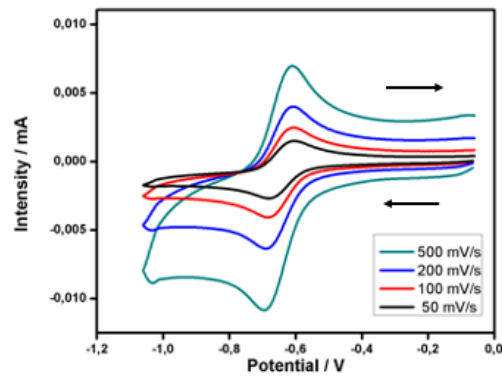
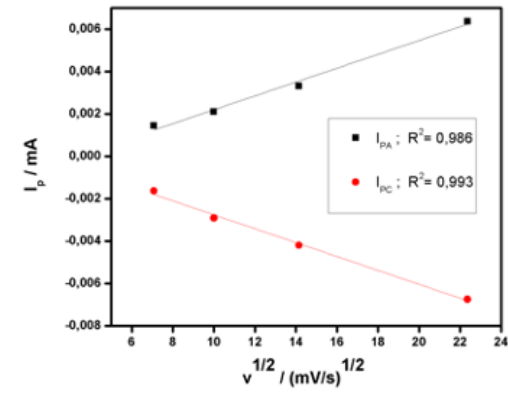
System	X	$\rho$	$\nabla^2\rho$	V	G	H	$ V /G$	D(A,B)
<b>1 hydrogen bond</b>	F	0.0069	0.0317	-0.0042	0.0061	0.0019	0.6885	0.0266
<b>1 X<math>\cdots\pi</math></b>		0.0044	0.0166	-0.0022	0.0032	0.0010	0.6875	0.0198
<b>1 C=O<math>\cdots\pi</math></b>		0.0050	0.0168	-0.0024	0.0033	0.0009	0.7273	0.0081
<b>2 hydrogen bond</b>	Cl	0.0059	0.0215	-0.0030	0.0042	0.0012	0.7143	0.0302
<b>2 X<math>\cdots\pi</math></b>		0.0064	0.0198	-0.0029	0.0039	0.0010	0.7436	0.0400
<b>2 C=O<math>\cdots\pi</math></b>		0.0055	0.0186	-0.0027	0.0037	0.0010	0.7297	0.0158
<b>3 halogen bond</b>	Br	0.0083	0.0331	-0.0049	0.0066	0.0017	0.7424	0.0773
<b>3 X<math>\cdots</math>H</b>		0.0058	0.0178	-0.0027	0.0036	0.0009	0.7500	0.0371
<b>3 <math>\pi\cdots\pi</math></b>		0.0067	0.0212	-0.0033	0.0043	0.0010	0.7674	0.0147
<b>4 halogen bond</b>	I	0.0109	0.0405	-0.0065	0.0083	0.0018	0.7831	0.1077
<b>4 X<math>\cdots</math>H</b>		0.0071	0.0193	-0.0032	0.0040	0.0008	0.8000	0.0500
<b>4 <math>\pi\cdots\pi</math></b>		0.0067	0.0210	-0.0033	0.0043	0.0010	0.7674	0.0147

# Electrochemical Studies

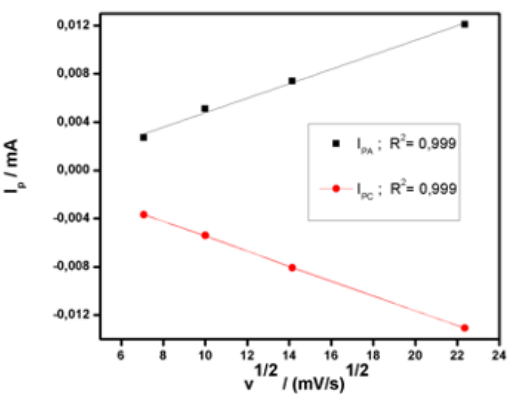
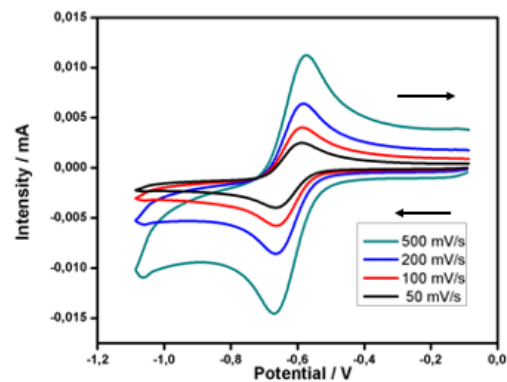
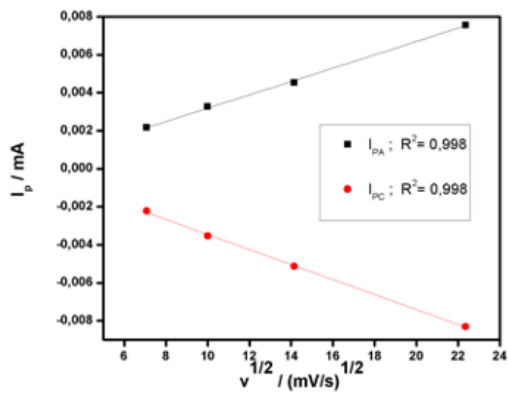
1



2



3



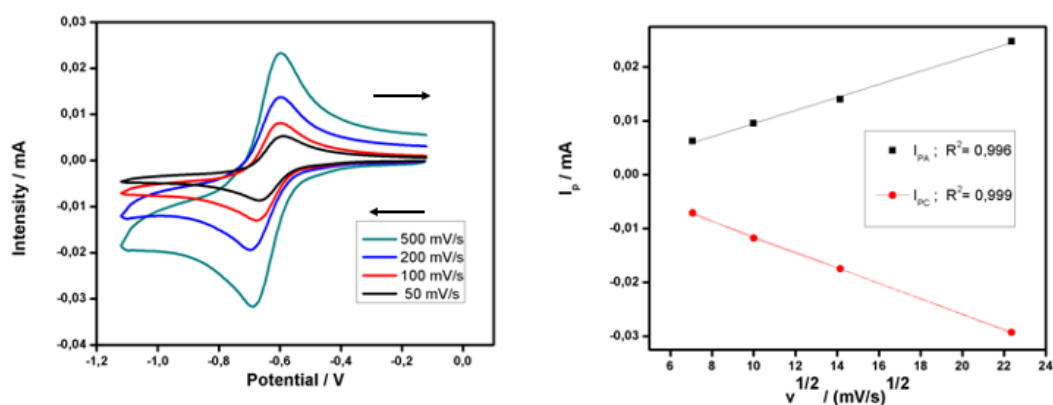


**Figure S8** Cyclic voltammogram ( $\text{Fe}^{3+}/\text{Fe}^{2+}$  redox peak) of **1-4** at different scan rates (left) and the representation of  $i_p$  vs  $v^{1/2}$  (right).

**Table S4** Electrochemical properties of **1-4**.

		$i_{pa}/i_{pc}$	$\Delta E_p$ (V)	$E^{\circ'}$ (V)	$D(\text{cm}^2 \cdot \text{s}^{-1})$
<b>1</b>	50 mV/s	0.856	0.063	-0.681	$5.31 \cdot 10^{-6}$
	100 mV/s	0.881	0.065	-0.675	
	200 mV/s	0.905	0.070	-0.683	
	500 mV/s	0.959	0.072	-0.682	
<b>2</b>	50 mV/s	0.967	0.066	-0.621	$6.43 \cdot 10^{-6}$
	100 mV/s	0.931	0.070	-0.622	
	200 mV/s	0.915	0.072	-0.622	
	500 mV/s	0.945	0.071	-0.623	
<b>3</b>	50 mV/s	0.869	0,066	-0.620	$1.68 \cdot 10^{-5}$
	100 mV/s	0.892	0.068	-0.615	
	200 mV/s	0.959	0.072	-0.618	
	500 mV/s	0.959	0.088	-0.619	
<b>4</b>	50 mV/s	0.911	0.068	-0.645	$7.56 \cdot 10^{-5}$
	100 mV/s	0.866	0.071	-0.642	
	200 mV/s	0.917	0.088	-0.644	
	500 mV/s	1.020	0.085	-0.644	

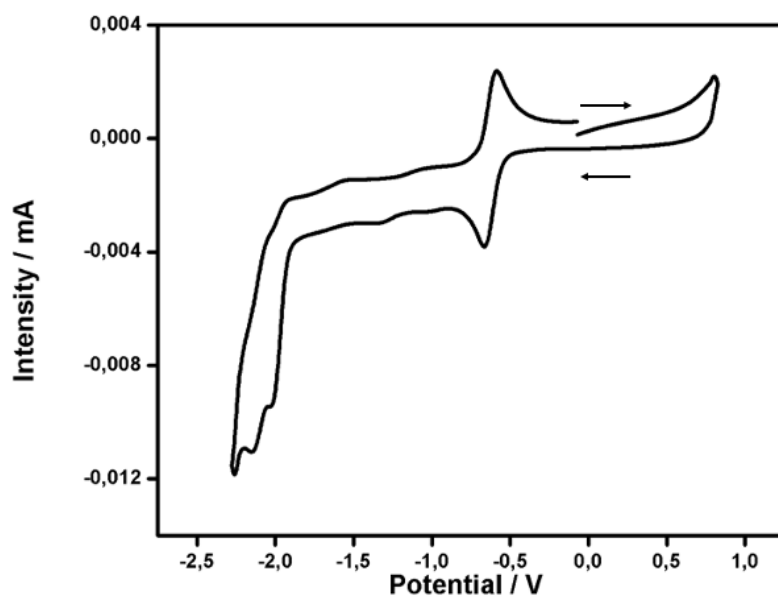


**Figure S9** Cyclic voltammogram of **4** in DCM containing 0.1 M of TBAPF<sub>6</sub> (scan rate 50 mV/s) vs Fc/Fc<sup>+</sup>.

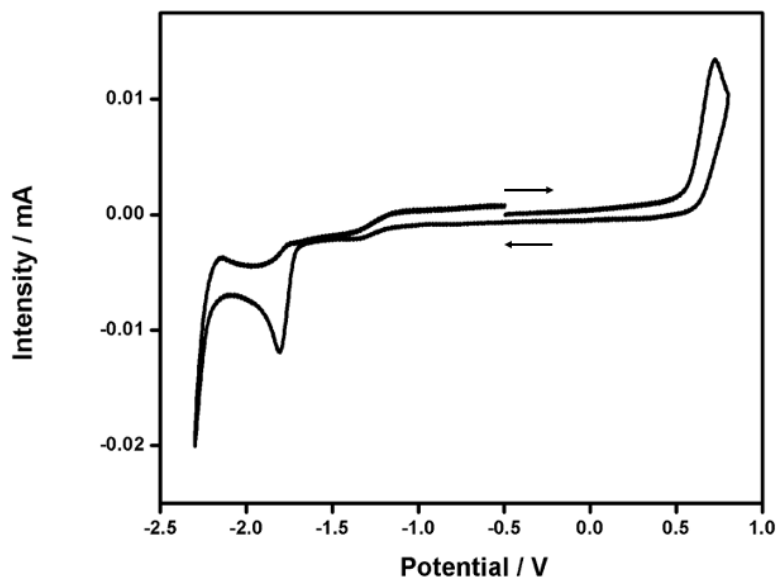


**Figure S10** Cyclic voltammogram of Hqsal-I in DCM containing 0.1 M of TBAPF<sub>6</sub> (scan rate 50 mV/s) vs Fc/Fc<sup>+</sup>.



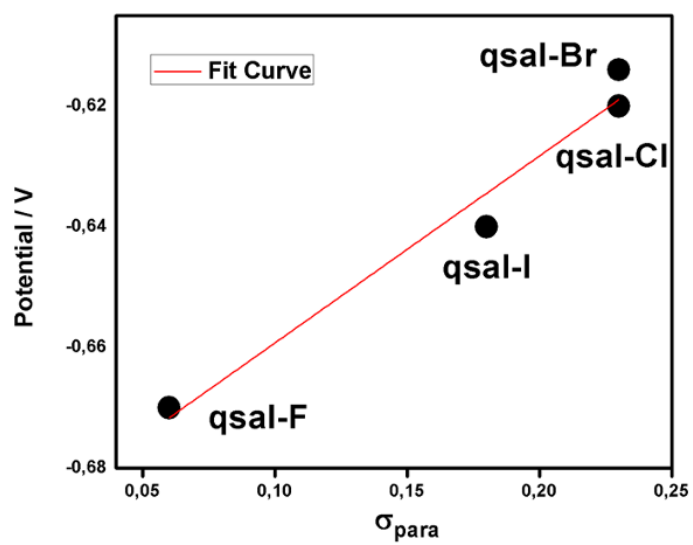


**Figure S11** Plot of  $E^{\circ}$ (V) vs  $\sigma_p$  for **1-4**.